

# An Ultra-Wideband Microwave Photonic Phase Shifter With a Full 360° Phase Tunable Range

Weilin Liu, *Student Member, IEEE*, Wangzhe Li, *Student Member, IEEE*, and Jianping Yao, *Fellow, IEEE*

**Abstract**—A novel photonic approach to the implementation of an ultra-wideband microwave phase shifter is proposed and experimentally demonstrated. In the proposed system, a single-sideband (SSB) signal is sent to a polarization-maintaining fiber Bragg grating (PM-FBG), which has two spectrally separated transmission notches along the fast and the slow axes. By locating the optical carrier in the SSB signal at the transmission notch, the optical carrier in the SSB signal is removed. At the output of the PM-FBG, two orthogonally polarized optical signals, one with the optical carrier and the sideband, the other with only the sideband, are obtained. The two orthogonal signals are then sent through a variable retardation plate (VRP) to a polarizer and then detected by a photodetector. By controlling the VRP to introduce a tunable phase difference between the two orthogonally polarized SSB signals, a microwave signal with a tunable phase shift is generated. A theoretical analysis is developed, which is validated by an experiment. A microwave phase shifter with a full 360° phase shift over a frequency range from 10 to 40 GHz is demonstrated.

**Index Terms**—Phase-shifted fiber Bragg grating, microwave photonics, microwave phase shifters, phased array beamforming, polarization.

## I. INTRODUCTION

MICROWAVE phase shifters (MPSs) are important devices for phased array beamforming in wireless communications [1], [2] and radar [3], [4] systems. MPSs are usually implemented based on semiconductors and ferrites [5], [6]. Semiconductor-based MPSs have high response speed, but the power-handling capacity is poor and the insertion losses are high [5]. On the contrary, ferrite-based MPSs have better power-handling capacity and the losses are smaller, but the response speed is limited and the size is usually large [6]. To implement MPSs with large bandwidth, small size and high response speed, photonic techniques are considered a solution. In the past few years, numerous photonic-assisted MPSs were proposed [7]–[11]. In [7], an MPS with a phase shift of 180° was realized based on cross-phase modulation (XPM) in a nonlinear loop mirror, in which the phase of the optical carrier of an optical single-sideband (SSB) signal is modulated via XPM [7]. The beating of the optical carrier and the sideband

generates a microwave signal with the phase shift translated to the microwave signal. In [8], an MPS with a phase shift of 135° based on wavelength conversion in a distributed feedback (DFB) laser was proposed. The fundamental principle of the technique is that a phase shift is introduced to a new wavelength during the wavelength conversion and the phase shift is tunable by controlling the injection current. Recently, MPSs based on slow- and fast-light effects in semiconductor optical amplifiers (SOAs) [9] or a tilted fiber Bragg grating (TFBG) [10] have been proposed. MPSs can also be realized based on stimulated Brillouin scattering (SBS) in a fiber [11]. The approaches reported in [7], [8], [10] have the limitation to provide a full 360° phase shift. Although the approach in [9] can achieve a full 360° phase shift, the system is complicated due to the use of multiple SOAs. The SBS-assisted microwave phase shifter can also provide a full 360° phase shift [11], [12], but to trigger the SBS, a high-power optical pump source is needed and the optical fiber is usually long. In addition, the SBS effect is sensitive to environmental change, which would affect the phase shift stability. Recently, Pan *et al.* proposed a simple technique to implement an MPS with a full 360° phase shift using a polarization modulator (PolM), an optical bandpass filter (OBPF) and a polarizer [13]. A PolM is a special phase modulator that supports TE and TM modes with complementary phase modulation indices [14]. By filtering out one sideband from each of the two orthogonally polarized phase-modulated signals using the OBPF, two SSB modulated signals that are orthogonally polarized are obtained. The phase shift is introduced by tuning the polarization direction of the polarizer. The major limitation of the approach is the need to generate two orthogonally polarized phase-modulated signals with complementary phase modulation. For many applications, however, a linearly polarized SSB modulated signal generated by a dual-port Mach–Zehnder modulator (MZM) is transmitted over an optical fiber. In addition, a  $\pi/2$  phase difference between the two orthogonally polarized signals at the output of the PolM is required, which is critical to the accuracy of the phase shift since a small drift of the bias voltage will have large impact on the phase shift accuracy. Thus, an electrical circuit to stabilize the bias voltage is needed, which may make the system more complicated.

In this letter, we propose and demonstrate a simple approach to implementing a microwave photonic phase shifter for a linearly polarized SSB modulated signal with a large bandwidth and a full 360° phase shift. In the proposed system, a linearly polarized SSB modulated signal is sent to a polarization-maintaining fiber Bragg grating (PM-FBG) through a

Manuscript received February 14, 2013; revised April 1, 2013; accepted April 23, 2013. Date of publication April 25, 2013; date of current version May 24, 2013. This work was supported in part by the Natural Science and Engineering Research Council of Canada.

The authors are with Microwave Photonics Research Laboratory, School of Electrical Engineering and Computer Science, University of Ottawa, Ottawa K1N 6N5, Canada (e-mail: jpyao@eecs.uOttawa.ca).

Color versions of one or more of the figures in this letter are available online at <http://ieeexplore.ieee.org>.

Digital Object Identifier 10.1109/LPT.2013.2260139

polarization controller (PC), to control the polarization direction of the incident light wave to have an angle of  $45^\circ$  relative to the fast axis of the PM-FBG. Thus, an identical power splitting along the fast and the slow axes is achieved. The optical carrier of the SSB signal along the fast axis is removed by the notch of the PM-FBG. Due to the birefringence, the notch of the PM-FBG along the slow axis is away from the notch along the fast axis, thus the SSB signal along the slow axis is not affected by the PM-FBG. By controlling the variable retardation plate (VRP) after the PM fiber, the two signals along the fast and slow axes will have a tunable phase difference. The optical signals at the output of the VRP are sent to a polarizer, and then detected by a photodetector (PD). A phase-shifted microwave signal is then generated. By adjusting the phase difference between the two orthogonal signals to the polarizer, the phase of the generated microwave signal is shifted. A theoretical analysis is performed, which is validated by an experiment. A microwave phase shifter with a full  $360^\circ$  phase shift over a frequency range from 10 to 40 GHz is experimentally demonstrated.

## II. PRINCIPLE

Fig. 1 shows the schematic of the proposed microwave phase shifter. It consists of a PC, a PM-FBG, a VRP, a polarizer and a PD. A linearly polarized SSB signal from a fiber link is sent to the PM-FBG via the PC, to adjust its polarization direction to have an angle of  $45^\circ$  relative to the fast axis of the PM-FBG. Two orthogonally polarized SSB signals are obtained at the output of the PM-FBG, with the optical carrier along the fast axis removed by the notch of the PM-FBG. The orthogonal SSB signals at the output of the VRP are combined at the polarizer and then detected at the PD. Depending on the phase difference between the two orthogonal SSB-modulated signals, a phase-shifted microwave signal with a tunable phase shift over a full  $360^\circ$  can be generated.

Mathematically, an SSB signal can be expressed as

$$E(t) = A \{ \exp(j\omega t) + \gamma \exp[j(\omega + \omega_m)t] \} \quad (1)$$

where  $A$  is the amplitude of the optical carrier,  $\omega$  and  $\omega_m$  are the angular frequencies of the optical carrier and the microwave signal, respectively, and  $\gamma$  is the modulation index. By applying the SSB signal to the PM-FBG with an angle of  $45^\circ$  relative to the fast axis of the PM-FBG, the SSB signal will be equally split and propagate along the fast and the slow axes of the PM-FBG. The PM-FBG has a notch along the fast and the slow axes. By aligning the optical carrier with the notch along the fast axis, the optical carrier is removed, as shown in Fig. 1, while the SSB signal along the slow axis is not affected. A tunable phase difference of the two orthogonal SSB signals is introduced by the VRP. At the output of the VRP, two orthogonally polarized signals with a phase difference of  $\varphi$  are obtained, which are given by

$$\begin{bmatrix} E_x \\ E_y \end{bmatrix} = \frac{\sqrt{2}}{2} A \begin{bmatrix} \gamma \exp[j(\omega + \omega_m)t - j\varphi] \\ \exp(j\omega t) + \gamma \exp[j(\omega + \omega_m)t] \end{bmatrix} \quad (2)$$

where  $E_x$  and  $E_y$  denote the electrical fields along the fast and slow axes, as shown in Fig. 1,  $\varphi$  is a tunable phase introduced

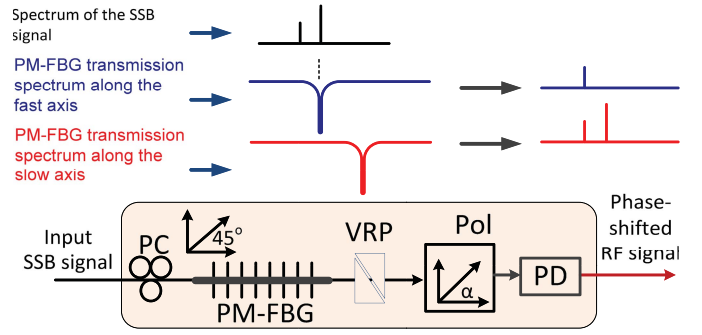


Fig. 1. Schematic of the proposed ultra-wideband  $360^\circ$  microwave photonic phase shifter. PC: polarization controller; SSB: single sideband; VRP: variable retardation plate; Pol: polarizer.

by the VRP. Note that the optical carrier along the  $x$  direction is removed. By adjusting the VRP, the phase difference of the incident signals to the VRP could be arbitrarily tuned. Thus, the signal at the output of the polarizer along its principal axis is given by

$$E_{out} = E_x \cos \alpha + E_y \sin \alpha \quad (3)$$

where  $\alpha$  and  $\pi/2 - \alpha$  are the angles between the principal axis of the polarizer and the two principal axes of the VRP. The signal in (3) is then sent to the PD for square-law detection, and the output current can be written as

$$\begin{aligned} I(t) &\propto E_{out}(t) E_{out}^*(t) \\ &= A_{DC} + A^2 \gamma \cos \alpha \sin \alpha \exp(j\omega_m t - j\varphi) \\ &\quad + A^2 \gamma \sin^2 \alpha \exp(j\omega_m t) \\ &= A_{DC} + A^2 \gamma \sin \alpha \left[ \cos \alpha \exp(j\omega_m t - j\varphi) \right. \\ &\quad \left. + \sin \alpha \exp(j\omega_m t) \right] \quad (4) \end{aligned}$$

where  $A_{DC}$  is the dc component. As can be seen the phase shift introduced to the microwave signal is a function of  $\varphi$  and  $\alpha$ . The amplitude of the microwave signal is also a function of  $\varphi$  and  $\alpha$ . For an ideal phase shifter, it is expected that the amplitude of the phase-shifted microwave signal is constant over the entire range of phase shift. To have a better understanding of the dependence of the microwave phase shift and the amplitude on  $\varphi$  and  $\alpha$ , a simulation is performed. For a given  $\alpha$ , we tune  $\varphi$  from  $-\pi$  to  $+\pi$ , the corresponding microwave phase shift is calculated, as shown in Fig. 2. As can be seen, a full  $360^\circ$  phase shift can be achieved for  $0 \leq \alpha \leq \pi/4$ . For  $\pi/4 < \alpha \leq \pi/2$ , the phase shift range is less than  $0.8\pi$ . Thus, to have a full  $360^\circ$  phase shift,  $\alpha$  should be selected to be within 0 to  $\pi/4$ .

Next, we investigate the output microwave power as a function of  $\alpha$  for  $0 \leq \alpha \leq \pi/4$ , with the result shown in Fig. 3(a). The power variation, defined as the difference between the maximum power and the minimum power for a full  $360^\circ$  phase shift or  $10 \log_{10}(P_{max}/P_{min})$ , is also calculated. As can be seen the variation is the smallest when  $\alpha = 0$ , but when  $\alpha = 0$ , the microwave power is 0. To have small power variation while maintaining a good output power, in our experiment  $\alpha$  is selected to be  $\pi/32$ , corresponding to a power variation within 1 dB, as shown in Fig. 3(a). Fig. 3(b) (solid line) shows the microwave phase shift as a function of  $\varphi$ , with the value

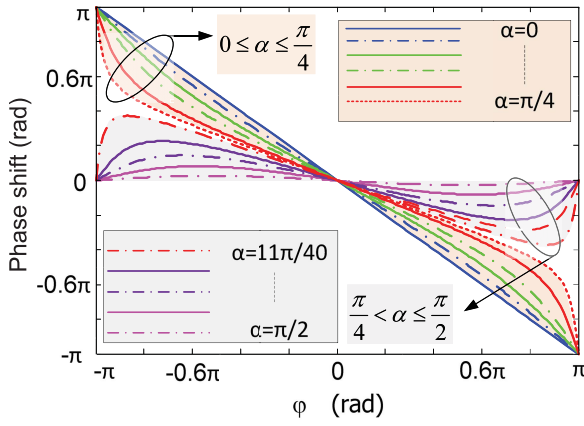


Fig. 2. Tunable microwave phase shift as a function of  $\phi$  for different  $\alpha$  from 0 to  $\pi/2$ .

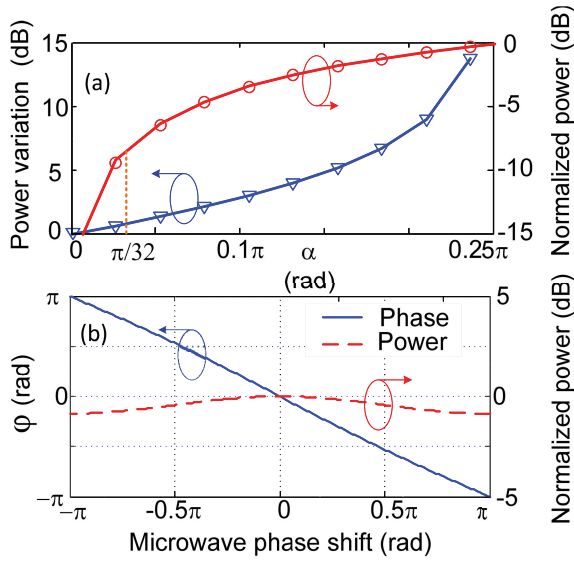


Fig. 3. (a) Microwave power variation and the received RF power as a function of  $\alpha$ . (b) Microwave phase shift and the microwave power variation as a function of  $\phi$  for  $\alpha = \pi/32$ .

of  $\alpha$  fixed at  $\pi/32$ . As can be seen the microwave phase shift has approximately a linear dependence on  $\phi$ . Thus, by tuning  $\phi$  from  $-\pi$  to  $+\pi$ , a full microwave phase shift of  $360^\circ$  is achieved. For the full  $360^\circ$  phase tuning, the power variation over the full phase tunable range is within 1 dB, as shown in Fig. 3(b) (dashed line).

### III. EXPERIMENT

An experiment based on the setup shown in Fig. 1 is implemented. A linearly polarized SSB modulated signal generated using an MZM followed by an optical notch filter to remove the upper sideband is sent to the PM-FBG through the PC. The notch filter is a WaveShaper (Finisar, WaveShaper 4000S) with a bandwidth of a 50 GHz and a notch rejection of 50 dB. By adjusting the incident angle to be  $45^\circ$  relative to the fast axis of the PM-FBG via tuning the PC, the SSB signal is projected equally to the fast and the slow axes of the PM-FBG. The optical carrier is controlled to locate at the notch of the PM-FBG along the fast axis which has a

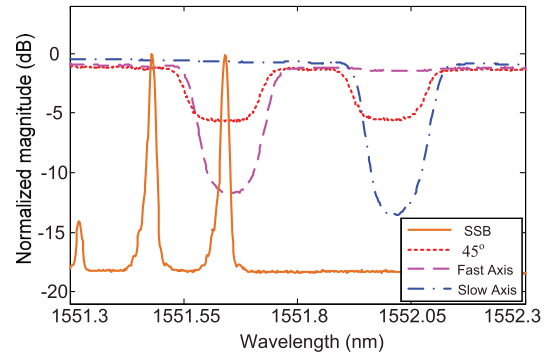


Fig. 4. Optical spectrum of the SSB signal and the transmission spectra of the PM-FBG measured when the incident light wave is aligned with the fast, slow axes of the PM-FBG, and with an angle of  $45^\circ$  relative to the fast axis. The frequency of the microwave signal is 20 GHz.

wavelength of 1551.64 nm, thus the optical carrier is filtered out along the fast axis. The spectrum of the SSB signal and the transmission spectra of the PM-FBG are both shown in Fig. 4. The transmission spectra of the PM-FBG are measured by aligning the polarization direction of the incident light parallel to the fast axis, the slow axis, and with  $45^\circ$  to the fast axis. Along the slow axis, the notch is shifted to a longer wavelength due to the birefringence of the PM fiber, thus both the optical carrier and the sideband transmit through the PM-FBG.

In the proposed system, the phase difference between the two orthogonal SSB signals is controlled by tuning the VRP. Due to the unavailability of the VRP, we use a second PC to introduce the phase difference in the experiment, and the angle  $\alpha$  is also controlled by the second PC. A phase-shifted microwave signal with its phase tunable by tuning the second PC is obtained at the output of the PD. Fig. 5 shows the phase shift measured using a vector network analyzer (VNA, Agilent E8364A). As can be seen a tunable phase shift from  $-180^\circ$  to  $180^\circ$  over a frequency range from 10 to 40 GHz is achieved. The lowest frequency is limited by the notch width of the PM-FBG and the highest frequency is limited by the bandwidth of the PD. To extend the frequency range, we may use a PM-FBG with a narrower notch width and a PD with a wider bandwidth.

The microwave power for different phase shift is also measured by the VNA, with the results shown in Fig. 6. As can be seen, the microwave powers over the range from 10 to 40 GHz at different phase shifts are maintained almost constant. The output power variations for the phase shift tuned at  $0^\circ$ ,  $-90^\circ$ ,  $+90^\circ$  and  $180^\circ$  over the frequency range from 10 to 40 GHz is within 1.27 dB, which is slightly higher than the theoretical value of 1 dB. In the experiment, the VRP is replaced by a second PC. When the second PC is tuned to introduce a phase shift, the angle  $\alpha$  is also changed. If the value of  $\alpha$  is not well maintained at  $\pi/32$ , an increased power variation would be resulted. If a commercial VRP is employed in the system, the power variation can be maintained within 1 dB.

The system performance, such as the gain, the noise figure, and the system stability, is also assessed. For an input RF power from  $-25$  to  $-10$  dBm, the averaged RF gain is measured to be  $-39.41$  dB. The link noise figure is also

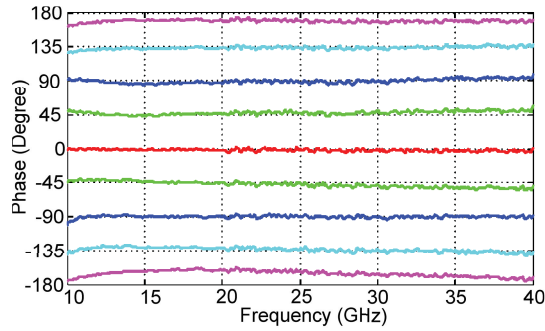


Fig. 5. Experimentally generated phase shift over a frequency range from 10 to 40 GHz.

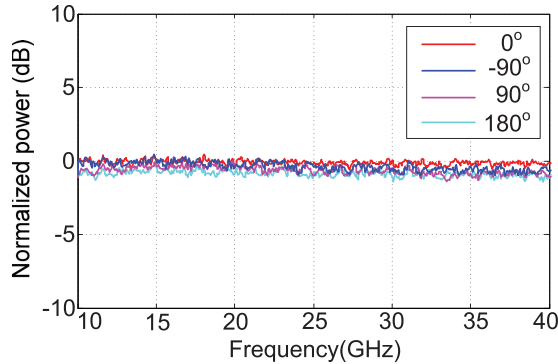


Fig. 6. Power of the phase-shifted microwave signal when achieving different phase shift over a frequency range from 10 to 40 GHz.

measured, which is 73.41 dB at a room temperature. The relatively large noise figure is due to the large noise floor of the electrical spectrum analyzer (ESA) used to perform the noise figure measurement, which is  $-140$  dBm/Hz. If an ESA with a lower noise floor, say  $-160$  dBm/Hz, is used, the link noise figure is then 53.41 dB. The long-term stability of the system is also evaluated. Under room environment, a phase variation within  $4.3^\circ$  is observed for a four-hour stability test.

#### IV. CONCLUSION

We have proposed and experimentally demonstrated a new approach to implementing a tunable phase shifter with a full  $360^\circ$  phase shift over an ultra-wide frequency range from 10 to 40 GHz. The key contribution of this technique is the ability of the system to introduce a tunable phase shift to any linearly polarized SSB signal using only passive components,

which greatly simplify the system and reduce the system noise and nonlinearity. The tunable phase shift was realized by simply tuning the VRP. The proposed technique was verified by an experiment. A microwave phase shifter with a full  $360^\circ$  phase shift over a frequency range from 10 to 40 GHz was demonstrated.

#### REFERENCES

- [1] A. Yamagashi, M. Ishikawa, T. Tsukahara, and S. Date, "A 2-V 2-GHz low-power direct digital frequency synthesizer chip set for wireless communication," in *Proc. IEEE CICC*, May 1995, pp. 319–322.
- [2] J.-L. Kuo, *et al.*, "60-GHz four-element phased-array transmit/receive system-in-package using phase compensation techniques in 65-nm flip-chip CMOS process," *IEEE Trans. Microw. Theory Tech.*, vol. 60, no. 3, pp. 743–756, Mar. 2012.
- [3] J. F. Coward, T. K. Yee, C. H. Chalfant, and P. H. Chang, "A photonic integrated-optic RF phase-shifter for phased-array antenna beam-forming applications," *J. Lightw. Technol.*, vol. 11, no. 12, pp. 2201–2205, Dec. 1993.
- [4] M. Attygalle and D. Stepanov, "Linear photonic technique for fixed and time varying RF phase shifts of radar signals," *Opt. Express*, vol. 20, no. 16, pp. 18025–18030, Jul. 2012.
- [5] H. Jacobs and M. M. Chrepta, "Electronic phase shifter for millimeter-wave semiconductor dielectric integrated circuits," *IEEE Trans. Microw. Theory Tech.*, vol. 22, no. 4, pp. 411–417, Apr. 1974.
- [6] A. B. Ustinov, G. Srinivasan, and B. A. Kalinikos, "Ferrite-ferroelectric hybrid wave phase shifters," *Appl. Phys. Lett.*, vol. 90, no. 3, pp. 031913-1–031913-3, Jan. 2007.
- [7] Y. Dong, H. He, and W. Hu, "Photonic microwave phase shifter/modulator based on a nonlinear optical loop mirror incorporating a Mach-Zehnder interferometer," *Opt. Lett.*, vol. 32, no. 7, pp. 745–747, Apr. 2007.
- [8] M. R. Fisher and S. L. Chuang, "A microwave photonic phase-shifter based on wavelength conversion in a DFB laser," *IEEE Photon. Technol. Lett.*, vol. 18, no. 16, pp. 1714–1716, Aug. 15, 2006.
- [9] W. Xue, S. Sales, J. Capmany, and J. Mørk, "Microwave phase shifter with controllable power response based on slow- and fast-light effects in semiconductor optical amplifiers," *Opt. Lett.*, vol. 34, no. 7, pp. 929–931, Apr. 2009.
- [10] H. Shahoei and J. P. Yao, "Tunable microwave photonic phase shifter based on slow and fast light effects in a tilted fiber Bragg grating," *Opt. Express*, vol. 20, no. 13, pp. 14009–14014, Jun. 2012.
- [11] A. Loayssa and F. J. Lahoz, "Broad-band RF photonic phase shifter based on stimulated Brillouin scattering and single-sideband modulation," *IEEE Photon. Technol. Lett.*, vol. 18, no. 1, pp. 208–210, Jan. 1, 2006.
- [12] M. Sagues and A. Loayssa, "Orthogonally polarized optical single sideband modulation for microwave photonics processing using stimulated Brillouin scattering," *Opt. Express*, vol. 18, no. 22, pp. 22906–22914, Oct. 2010.
- [13] S. Pan and Y. Zhang, "A tunable and wideband microwave photonic phase shifter based on a single sideband polarization modulator and a polarizer," *Opt. Lett.*, vol. 37, no. 21, pp. 4483–4485, Nov. 2012.
- [14] J. D. Bull, N. A. F. Jaeger, H. Kato, M. Fairburn, A. Reid, and P. Ghanipour, "40 GHz electro-optic polarization modulator for fiber optic communication systems," *Proc. SPIE*, vol. 5577, pp. 133–143, Dec. 2004.